ChemComm

Accepted Manuscript

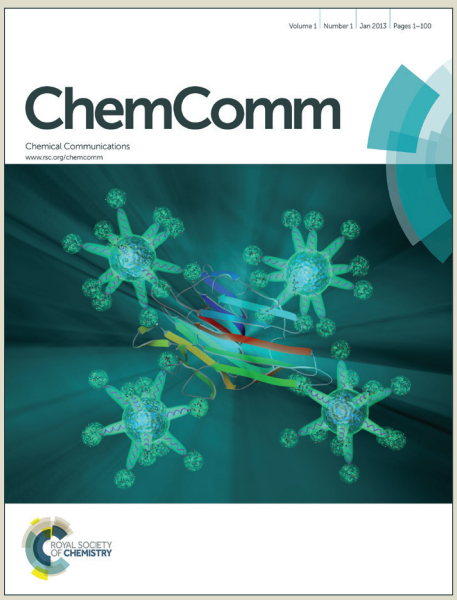

ROYAL SOCIETY OF CHEMISTRY

www.rsc.org/chemcomm

Journal Name

RSCPublishing

COMMUNICATION

Nanovalve Activation by Surface-Attached Photoacids

Cite this: DOI: 10.1039/xoxxoooooox

T. M. Guardado-Alvarez,[a] M. M. Russell[a] and J. I. Zink[a*]

Received ooth January 2012,
Accepted ooth January 2012

DOI: 10.1039/xoxxoooooox

www.rsc.org/

Proton transfer caused by excitation of a photoacid attached to the surface of a mesoporous silica nanoparticle activates a nanovalve and causes release of trapped molecules. The protonation of an aniline- based stalk releases a noncovalently bound cyclodextrin molecule that blocked a pore. The results show that pH-responsive molecular delivery systems can be externally controlled using light.

Photoacids, molecules that have an excited electronic state pK_a much lower than that in their ground state, have proven useful and important in fundamental studies of proton transfer.[1, 2] Because the acidification is relatively localized in the vicinity of the photoacid, acid-induced polymerization can be used in photolithography and the production of photoresists.[3] Other than their transient state as photoacids, they completely resemble ground state protic acids.[2, 4, 5] Using photoacids, the dynamics of proton transfer can be studied in bulk solutions, in confined spaces[6, 7] and on surfaces using time-resolved spectroscopy and optical pump-probe techniques.[3, 5, 8,]

Pyrene-based compounds are an important class of photoacids and have been studied extensively. It has been shown that these molecules have a geminate recombination that is reversible. For example 8-hydroxypyrene-1,3,6-trisulfonate (HPTS) has a ground state pKa of 8.1 that decreases to 1.6 in its excited state.[4] The rate of recombination of protons with HPTS in the pores of sol-gel matrices was studied.[9] A closely related molecule, 6,8-dihydroxy-1,3-pyrenedisulfonic acid disodium salt (DHDS) the photoacid that is used in this study, has an additional -OH group that is used as the reactive group for the attachment to silica. The photoacidic properties and excited state pKa of DHDS when one of the OH groups has been functionalized are very similar to those of HPTS.[10]

In this communication we show that photoexcitation of DHDS can activate a nanovalve on a mesoporous silica nanoparticle (MSN) by proton transfer. The photoacid is covalently attached to the surface of MSNs next to an acid-activated nanovalve (Fig. 1) that consists of an aniline based molecule (stalk) with a pH-dependent binding constant with α-cyclodextrin (α-CD). The α-CD functions as a bulky group that is able to cap the nanopores when the stalk is uncharged, preventing the cargo from escaping. Upon protonation of the stalk, the α-CD is detached and the cargo is released. The nanovalve was chosen to have a pKa of ~6 (Stalk1, Figure 2a),

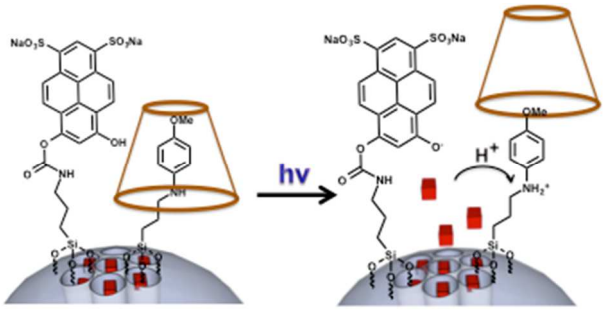

Fig. 1. Sketch of the photoacid and the cyclodextrin-capped stalk on the surface of a MSN. Photoactivation causes local acidification that protonates the stalk and releases the cyclodextrin and the trapped cargo molecules.

which will allow the system to remain closed in a neutral environment, while being sensitive enough to respond to acidification by the photoacid.[11]

The MSNs with a two-dimensional hexagonal pore structure were synthesized using a sol gel method[11-17] and the stalks were attached as previously described.[11] DHDS was reacted with 3-isocyanatopropyltriethoxysilane (ICPES) and then condensed onto the MSNs surface. The cargo was loaded by soaking the particles in a concentrated solution of propidium iodide (PI) and allowing it to diffuse into the pores. The α-CD stopper was threaded on the stalk blocking the pores and preventing the cargo from escaping. Upon irradiation at 408 nm, DHDS protonates the stalk causing the α-CD to dethread and allowing the release of the PI cargo (Fig. 1).

Characterization of the system was done using multiple methods. The MSNs were characterized using powder X-ray diffraction (pXRD) and transmission electron microscopy (TEM). From the TEM studies, the pore diameter was found to be around 2.5 nm and the particle size between 50 to 100 nm (Fig S1). From the pXRD the higher order peaks observed can be indexed as the (1 0 0), (1 1 0) and (2 0 0) planes with a lattice spacing of 4 nm. The N_2 absorption-desorption isotherms showed a specific surface of 1044 m^2 / g. The attachment of the DHDS was confirmed by fluorescence spectra of

the DHDS-MSNs showing an emission peak at around 450 nm from the DHDS molecule (Fig. S3). An infrared spectrum of the DHDS-MSNs was also taken showing a stretch at around 1300 cm^{-1} corresponding to the asymmetric sulfonate stretch (Fig. S4). The attachment of stalk1 was confirmed using UV-Vis which showed an absorption peak at around 300 nm consistent with the aniline absorption (Fig. S2). The DHDS to valve ratio was approximately 1:1 based on UV-Vis spectroscopy.

The system was tested using continuous monitoring of the fluorescence of the cargo released; unless otherwise stated all experiments where carried out in DI water. The particles were placed in a corner of a one by two centimeter glass cuvette. DI water was then carefully added to the cuvette without disturbing the particle precipitate. On the opposite side of the cuvette, a small stirring magnet was placed to aid in the distribution of the PI that is released from the particles. The fluorescence intensity excited by a 448 nm probe beam was monitored over time. In order to excite the photoacid, a 408 nm (10 mW) pump beam was directed onto the particles.

The experimental results showed that the system remains closed at neutral pH; the fluorescence intensity does not increase when the pump beam is off. After 45 minutes the 408 nm pump beam was turned on causing the photoacid to protonate stalk1 and thus dissociate the α-CD. An immediate increase in the fluorescence intensity was observed, indicating that the PI was released from inside the MSNs nanopores and into solution as shown in Fig. 2a. Even though there is no overall detectable pH change in solution, the local pH on the surface of the MSNs becomes acidic.

As a control experiment the system was tested in a solution buffered at pH 8 using a TRIS buffer and the experimental set up previously described. As expected, the results showed that when the solvent is buffered the proton dissociation from the photoacid is unable to significantly change the local pH on the surface of the MSNs, preventing acidification and nanovalve opening (Fig. 2a).

To test the on command activation of the system an experiment was conducted where the pump laser was repetitively turned on and off. When the pump beam is turned off, the proton returns to the DHDS and the pH on the MSNs surface becomes neutral. In this experiment the pump laser was first kept off to establish a baseline. After 30 minutes the 408 nm pump laser was turned on and an immediate increase in fluorescence intensity from the release of PI was observed. After 90 minutes, the pump laser was turned off. The rate of release immediately decreased showing that the local pH returned to neutral, no more stalks were being protonated, and the uncapping of the remaining nanovalves was stopped as shown in Fig. 2b. The fluorescence intensity continued to increase slightly over time during the off cycle due to the slow diffusion of PI out of the pores that had been uncapped during the excitation. The on-off sequence was repeated and the same trend was observed. These results show that the system can be controlled temporally and that the dose of released cargo molecules can also be controlled externally.

A control experiment was done to prove that the absorbed photons from the pump beam and not simply local heating was the cause for the dissociation of α-CD from stalk1. The pump wavelength was changed to 514 nm, a wavelength where the DHDS has no absorptivity and thus is unable to be excited and transfer a proton to stalk1. The power used was 50 mW which is five times greater than that of the 10 mW, 408 nm pump. The same experimental sequence was carried out; the pump beam was left off to establish a base line, and after 20 minutes the 514 nm pump beam was turned on. No change in the fluorescence intensity was observed. Then, in order to prove that the system was still functional when the right excitation wavelength was used, the 408 nm beam

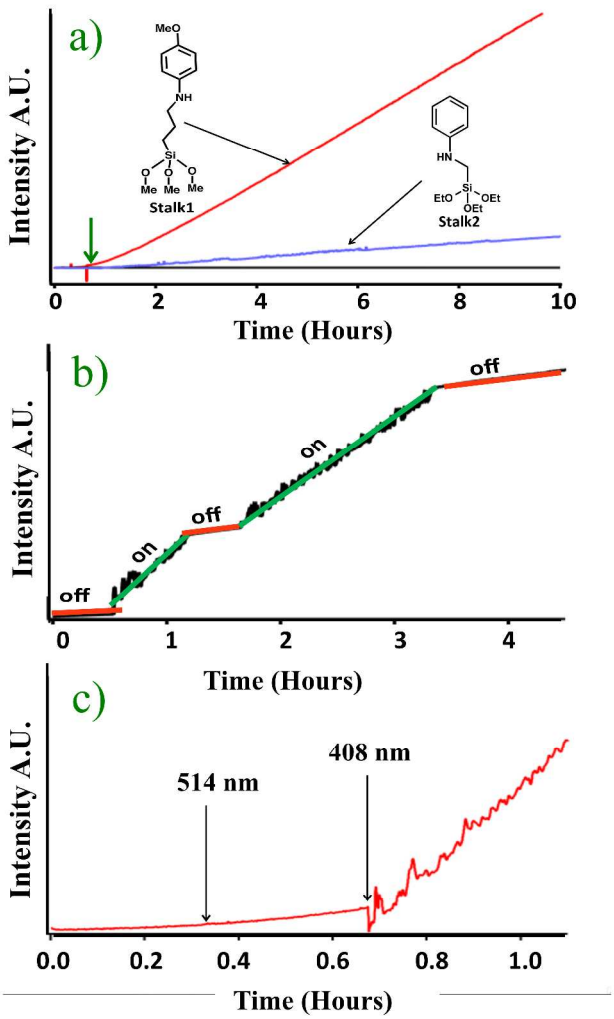

Fig. 2. a) Continuous monitoring of the photoacid-activated release of propidium iodide from particles containing Stalk1 (upper trace) and Stalk2 (middle trace). No photoactivation occurs in TRIS buffer (bottom trace). The 10 mW, 408 nm pump laser was turned on at 40 minutes (vertical arrow). b) Release profile from the Stalk1 system activated by sequential on/off cycles. The 10 mW, 408 nm pump laser was used. c) Wavelength dependence of nanovalve activation of the Stalk1 system. At 0.4 hours the 514 nm (50 mW) pump laser excitation was turned on for 20 minutes, and then at 0.75 hours the 408 nm (10 mW) pump laser was turned on.

was turned on. Immediately after this, an increase in the fluorescence intensity of the PI was measured (Fig. 2c).

This system can alternatively be activated by acidification of the bulk solvent. Setting up the experiment as previously described, the pump beam was left off for 20 minutes to establish a baseline, the 408 nm pump laser was then turned on and the fluorescence intensity showed an immediate increase. About 2 hours later the pump beam was turned off and the solution was acidified to pH 5 by the addition of HCl. The fluorescence continued to increase as shown in Fig. 3a. For comparison purposes, the activation of the stalk1-MSNs (no DHDS on the surface) when the bulk solution pH is lowered to 5 is shown in Fig. 3b. These results showed that the local pH change on the MSN caused by the photoacid had an effect on the nanovalve similar to that of bulk acidification of the solution to pH 5. The total

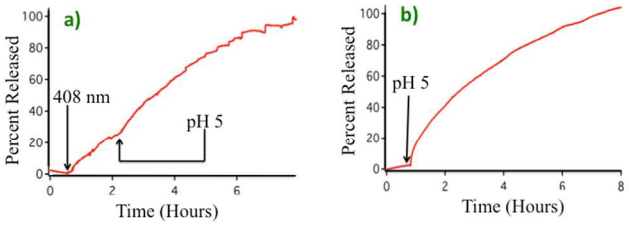

Fig. 3. Comparison between photoacid and bulk acidification on the release profiles. a) Release profile caused by 10 mW, 408 nm pump laser photoactivation for two hours, followed by solution acidification to pH 5. Both traces are on the same scale. b) Release profile caused by bulk acidification to pH 5 using HCl.

amount of dye released at the conclusion of this experiment was 2.8 wt%.

The experimental verification of the activation of the nanovalve by the photoacid shows that in a localized volume on the nanoparticle surface that contains chemically bonded photoacids and nanovalves, there are enough protons available to protonate stalks and dissociate cyclodextrin molecules. A simple order of magnitude calculation provides a more quantitative picture. Based on the surface coverage, the average distance between a photoacid molecule and a stalk on a nanoparticle's surface is about 1 nm. From measured hydrodynamic radii, a conservative estimate of the vertical distance from the surface of associated water molecules is 10 nm. Thus the volume of the cylinder with a radius of 1 nm and a length of 10 nm is 31 nm^3 or 1.26 10^{-22} L.[17] The pH in this volume when the photoacid is excited is thus about 2.2

Because the calculated pH value on the surface of the nanoparticle is much lower than the pK of the valve, a new system was synthesized using stalk2 shown in Fig. 2a to verify that the photoacid would open a nanovalve that requires a lower pH for activation. Stalk2 was chosen because it was previously reported to require a pH of ~3.5 in order to open.[11] The new system was prepared using same procedures as those used for stalk1, and it was tested for release as previously described. A baseline was taken for 40 minutes, after which the 408 nm pump laser was turned on. An increase in fluorescence intensity was observed indicating the opening of the valve and release of the dye as shown in Fig. 2a. As expected, the rate of release from the stalk2 is slower than that from the stalk1 valve because the pK is much lower.

Conclusions

In summary we have shown that the photoexcitation of DHDS can activate a nanovalve on a mesoporous silica nanoparticle by proton transfer. Control experiments were conducted to verify that the activation mechanism is via proton transfer. Calculations were made that suggest the local pH at the nanoparticle surface during exposure to light is around 2. An additional experiment was conducted using a different nanovalve that opens at a lower pH demonstrating the photoacid can activate a wide range of pH sensitive systems. To our knowledge this represents the first example of a photoacid-activated molecular machine on silica nanoparticles. This system is an example of an amplified signal probe for proton transfer because each pore opening event releases multiple fluorescent molecules. It also demonstrates that existing pH sensitive delivery systems[18-20] can be reconfigured for light activation.

This research was supported by the NIH RO1 CA133697, by the Defense Threat Reduction Agency HDTRA1-13-1-0046, and by a NIH fellowship to Tania Maria Guardado-Alvarez.

Notes and references

[a]*Department of Chemistry and Biochemistry and California NanoSystems Institute, University of California, Los Angeles, California 90095-1569.*

Electronic Supplementary Information (ESI) available: TEM of MCM-41, powder XRD of MCM-41, UV-vis spectra, Emission Spectrum, IR spectrum. See DOI: 10.1039/c000000x/

1 W.H. Thompson, *Ann. Rev. Phys. Chem.,* 2011, **62,** 599
2 S. J. Formosinho and L.G. Arnaut, *J. Photochem. Photobiol. A: Chem.,* 1993, **75,** 21
3 Y. Funchs, O. Soppera and K. Haupt, *Anal. Chim. Acta.*, 2012, **7**, 20.
4 S. Y. Goldberg, E. Pines and D. Huppert, *Chem. Phys. Lett.*, 1992, **192**, 77.
5 J. McKiernan, E. Simoni, B. Dunn and J. I. Zink, *J. Phys. Chem.*, 1994, **98**, 1006.
6 S.-Y. Park, H. Jeong, H. Kim, J. Y. Lee and D.-J. Jang, *J. Phys. Chem. C*, 2011, **115**, 24763
7 H. P. Soroka, R. Simkovitch, A. Kosloff, S. Shomer, A. Pevzner, O. Tzang, R. Tirosh, F. Patolsky and D. Huppert, *J. Phys. Chem. C*, 2013, **117**, 25786.
8 M. Gutman, D. Huppert and E. Pines, *J. Am. Chem. Soc*., 1981, **103**, 3709.
9 M. H. Huang, B. S. Dunn and J. I. Zink, *J. Am. Chem. Soc*., 2000, **122**, 3739.
10 H. R. Kermis, Y. Kostov and G. Rao, *Analyst*, 2003, **128**, 1181.
11 L. Du, S. Liao, H. A. Khatib, J. F. Stoddart and J. I. Zink, *J. Am. Chem. Soc*., 2009, **131**, 15136.
12 Z. Li, J. C. Barnes, A. Bosoy, J. F. Stoddart and J. I. Zink, *Chem. Soc. Rev.*, 2012, **41**, 2590.
13 M. W. Ambrogio, C. R. Thomas, Y.-L. Zhao, J. I. Zink and J. F. Stoddart, *Acc. Chem. Res.*, 2011, **44**, 903.
14 Y. Yang, W. Song, A. Wang, P. Zhu, J. Fei and J. Li, *PCCP*, 2010, **12**, 4418.
15 S. Angelos, M. Liong, E. Choi and J.I. Zink, *Chem. Eng. J.*, 2008, **137**, 4.
16 H. Meng, M. Xue, T. Xia, Y.-L. Zhao, F. Tamanoi, J. F. Stoddart, J. I. Zink and A. E. Nel, *J. Am. Chem. Soc*. 2010, **132**, 12690.
17 M. Xue and J. I. Zink, *J. Phys. Chem. Lett*., 2013, **52**, 2044.
18 D. Tarn, M. Xue. and J.I. Zink, *Inorg. Chem.,* 2009, **131**, 1686.
19 Y. Qiu, and K. Park, *Adv. Drug Deliv. Rev.,* 2012, **64,** 49.
20 M. Xue, D. Cao, J.F. Stoddart and J.I. Zink, *Nanoscale*, 2012,**4**, 7569.